The following Communications have been judged by at least two referees to be "very important papers" and will be published online at www.angewandte.org soon:

*A. V. Zabula, S. N. Spisak, A. S. Filatov, A. Y. Rogachev, M. A. Petrukhina**
Strain-Releasing Trap for Highly Reactive Electrophiles: Structural Characterization of Bowl-Shaped Arenium Carbocations

*A. Nagy, J. Fulara, I. Garkusha, J. P. Maier**
On the Benzylium/Tropylium-Ion Dichotomy: Electronic Absorption Spectra in Neon Matrices

*H. C. S. Chan, J. Kendrick, F. J. J. Leusen**
The Tale of Molecule VI, a Benchmark Sulfonimide for Crystal-Structure Prediction: Are Its Polymorphs Predictable?

*R. P. Sonawane, V. Jheengut, C. Rabalakos, R. Larouche-Gauthier, H. K. Scott, V. K. Aggarwal**
Enantioselective Construction of Quaternary Stereogenic Centers from Tertiary Boronic Esters: Methodology and Applications

X. Lang, H. Ji, C. Chen, W. Ma, J. Zhao**
Selective Formation of Imines by Aerobic Photocatalytic Oxidation of Amines on TiO_2

*K. Press, Ad Cohen, I. Goldberg, V. Venditto, M. Mazzeo, M. Kol**
Salalen–Titanium Complexes for the Highly Isospecific Polymerization of 1-Hexene and Propylene

*K. Nakano, S. Hashimoto, M. Nakamura, T. Kamada, K. Nozaki**
Synthesis of Stereogradient Poly(propylene carbonate) by Stereo- and Enantioselective Copolymerization of Propylene Oxide with Carbon Dioxide

D. Portehault, S. Devi, P. Beaunier, C. Gervais, C. Giordano, C. Sanchez, M. Antonietti*
A General Solution Route toward Metal Boride Nanocrystals

*K. Ohmori, T. Shono, Y. Hatakoshi, T. Yano, K. Suzuki**
An Integrated Synthetic Strategy for Higher Catechin Oligomers

L. Aboshyan-Sorgho, C. Besnard, P. Pattison, K. R. Kittilstved, A. Aebischer, J.-C. Bünzli, A. Hauser, C. Piguet**
Molecular Near-Infrared to Visible Light Upconversion in a Trinuclear d–f–d Complex

*R. Kaminker, R. Popovitz-Biro, M. E. van der Boom**
Coordination-Polymer Nanotubes and Spheres: A Ligand-Structure Effect

Author Profile

Rüdiger Kniep ____ **2670**

"My favorite subject at school was fine arts. When I was eighteen I wanted to be an architect. …"
This and more about Rüdiger Kniep can be found on page 2670.

Highlights

Core–Shell Electrocatalysts

H. Yang* ____ **2674–2676**

Platinum-Based Electrocatalysts with Core–Shell Nanostructures

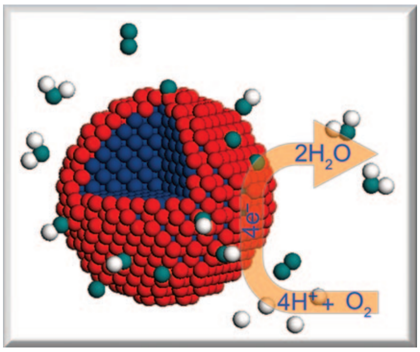

The core of the problem: Electrocatalysts need to be highly active and durable under harsh reactive environments in order to meet the requirements for future automotive applications. Platinum-group-metal-based core–shell and core–shell-like nanostructures have great potential in the design of multifunctional catalysts for the oxygen reduction reaction (ORR; see picture).

Contents

Metastability

C. J. Shaffer, D. Schröder* 2677 – 2678

The Demise and Revival of Diazirinone

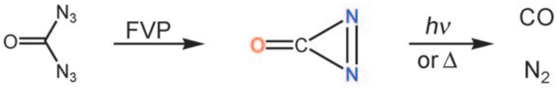

Experiments in existentialism: Diazirinone is a molecule with a colorful history. Once considered a transient species, it was recently recast as an elusive species. That "death announcement" is no longer appropriate, as the recent synthesis and flash vacuum pyrolysis (FVP) of carbonyl diazide has resulted in the first synthesis and full spectroscopic characterization of diazirinone.

Minireviews

Drug Design

G. M. Popowicz, A. Dömling, T. A. Holak* 2680 – 2688

The Structure-Based Design of Mdm2/Mdmx–p53 Inhibitors Gets Serious

Targeted nongenotoxic tumor therapy is an emerging and promising field of pharmacology. Understanding the cellular mechanism involved in tumorigenesis enables researchers to regulate the molecular machinery responsible for DNA repair and cell-cycle control. Structural data are crucial for the development of such novel nongenotoxic drug leads, which should help cells in the fight against cancer.

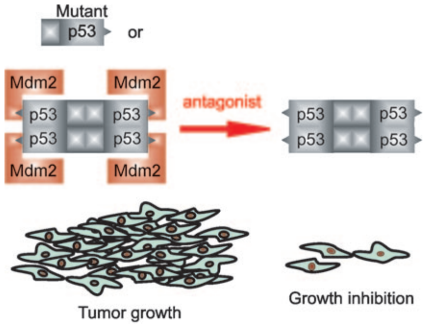

Reviews

Finite-Time Thermodynamics

B. Andresen* 2690 – 2704

Current Trends in Finite-Time Thermodynamics

The essential element of thermodynamic optimization is to coax a system (the horse) along the optimal path by interaction with a judicially varying reservoir (the moving carrot). This is called a horse–carrot process. If the distance from the horse to the carrot is small the horse will not move very quickly; if the distance is too large, it will give up and not move at all. The goal of optimization is to find the right driving force under the given conditions.

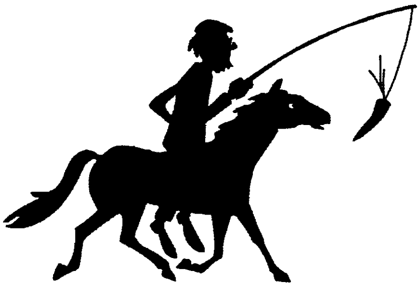

For the USA and Canada: ANGEWANDTE CHEMIE International Edition (ISSN 1433-7851) is published weekly by Wiley-VCH, PO Box 191161, 69451 Weinheim, Germany. Air freight and mailing in the USA by Publications Expediting Inc., 200 Meacham Ave., Elmont, NY 11003. Periodicals postage paid at Jamaica, NY 11431. US POSTMASTER: send address changes to *Angewandte Chemie*, Journal Customer Services, John Wiley & Sons Inc., 350 Main St., Malden, MA 02148-5020. Annual subscription price for institutions: US$ 9442/8583 (valid for print and electronic / print or electronic delivery); for individuals who are personal members of a national chemical society prices are available on request. Postage and handling charges included. All prices are subject to local VAT/sales tax.

Communications

Contractually binding: The methionine residues of the extracellular domain of hCTR1 (hCTR1_*N*) and its mutants were shown to be the key residues for cisplatin binding. hCTR1_*N* significantly facilitates the activation of the drug by the formation of Pt–thioether species. The anticancer drug is likely transported by hCTR1 through methionine-based sulfur–sulfur exchange (see picture).

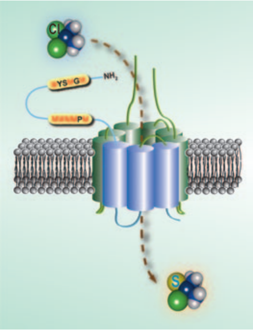

Drug–Protein Adducts

X. Wang, X. Du, H. Li, D. S.-B. Chan, H. Sun* ______ **2706–2711**

The Effect of the Extracellular Domain of Human Copper Transporter (hCTR1) on Cisplatin Activation

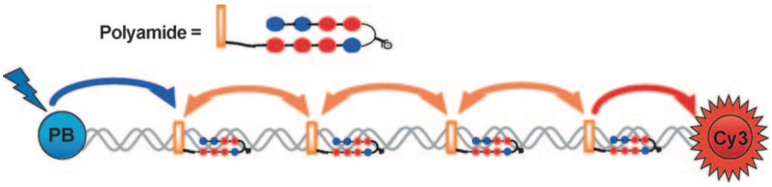

Relay race: The first example of a programmable DNA photonic wire is reported utilizing fluorophore-tethered pyrrole-imidazole polyamides for site-directed fluorophore assembly along a pre-formed DNA duplex (see scheme; PB = Pacific Blue, Cy3 = Cyanine 3; orange rectangles = fluorophore). The importance of such control is revealed by efficient energy transport over distances in excess of 27 nm.

DNA Photonics

W. Su, M. Schuster, C. R. Bagshaw, U. Rant,* G. A. Burley* ______ **2712–2715**

Site-Specific Assembly of DNA-Based Photonic Wires by Using Programmable Polyamides

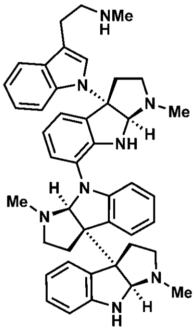

psychotetramine

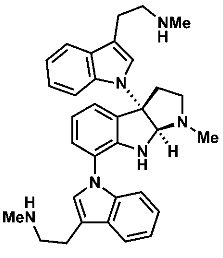

psychotrimine

Solving the puzzles: Total synthesis played a key role in the elucidation of the stereochemistry and verification of the constitution of the complex polymeric natural product psychotetramine. The route features three powerful assembly processes that enabled four rounds of total synthesis-guided structure determination. The pursuit of this alkaloid also led to an improved procedure for indole–aniline coupling and a highly efficient enantioselective synthesis of psychotrimine.

Natural Product Synthesis

K. Foo, T. Newhouse, I. Mori, H. Takayama, P. S. Baran* ______ **2716–2719**

Total Synthesis Guided Structure Elucidation of (+)-Psychotetramine

C–H Activation

F. E. Zilly, J. P. Acevedo, W. Augustyniak, A. Deege, U. W. Häusig, M. T. Reetz* ———— 2720 – 2724

Tuning a P450 Enzyme for Methane Oxidation

A new spin: The addition of chemically inert perfluoro carboxylic acids (green; see picture) to P450 enzymes results in dramatic activation of their catalytic activity as a result of the conversion of the Fe/heme from a low-spin to a high-spin state, and the reduction of the binding-pocket size. Together these effects allow otherwise inert substrates such as propane and even methane to be oxidized.

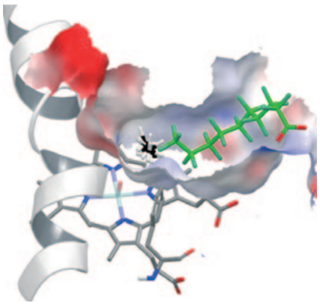

Phthalocyanines

T. Honda, T. Kojima,* N. Kobayashi,* S. Fukuzumi* ———— 2725 – 2728

Crystal Structures and Electronic Properties of Saddle-Distorted and Protonated Phthalocyanines

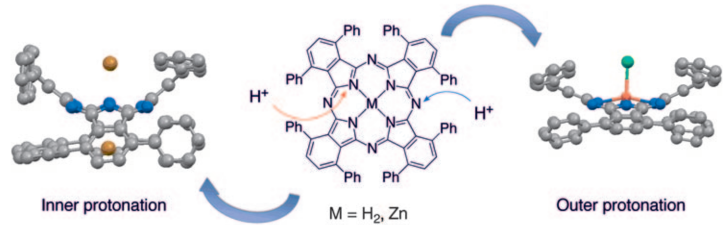

Protonation made easy: The formation and crystal structure determination of phthalocyanine protonated at the *meso*- and isoindole nitrogen atoms (see picture) are achieved by using the free base and a zinc complex of saddle-distorted octaphenylphthalocyanine, respectively. The saddle deformation alters the electronic structure of the phthalocyanine ring and facilitates its protonation.

Electrocatalysis

L. Liu,* E. Pippel ———— 2729 – 2733

Low-Platinum-Content Quaternary PtCuCoNi Nanotubes with Markedly Enhanced Oxygen Reduction Activity

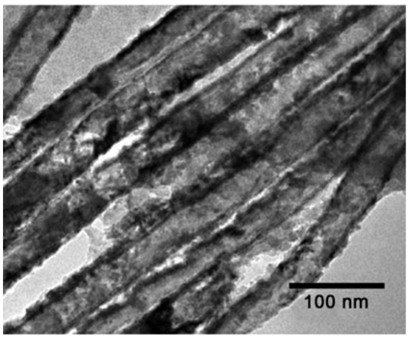

The title nanotubes were synthesized by template-assisted one-step electrodeposition and found to exhibit markedly enhanced electrocatalytic activity toward oxygen reduction, which can be attributed to a combination of several favorable factors: the multicomponent nature with which different elements work synergistically, the strain and electronic effects associated with surface dealloying, and their hollow and porous geometry.

Heterocycles

T. C. Coombs, G. H. Lushington, J. Douglas, J. Aubé* ———— 2734 – 2737

1,3-Allylic Strain as a Strategic Diversification Element for Constructing Libraries of Substituted 2-Arylpiperidines

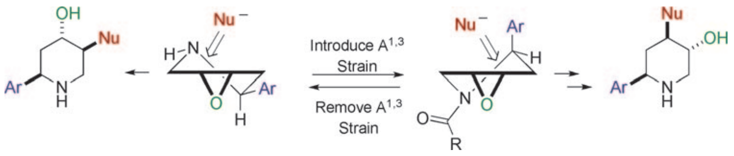

Flipping diversity: Minimization of 1,3-allylic strain ($A^{1,3}$ strain) is a recurring element in the design of a stereochemically and spatially diverse collection of 2-arylpiperidines. $A^{1,3}$ strain guides the regioselective addition of nucleophiles and N-substituents leverage $A^{1,3}$ strain to direct each stereoisomer to two different conformer populations, thus doubling the number of library members.

Microspheres

X. Lai, J. Li, B. A. Korgel, Z. Dong, Z. Li, F. Su, J. Du, D. Wang* ____ **2738 – 2741**

General Synthesis and Gas-Sensing Properties of Multiple-Shell Metal Oxide Hollow Microspheres

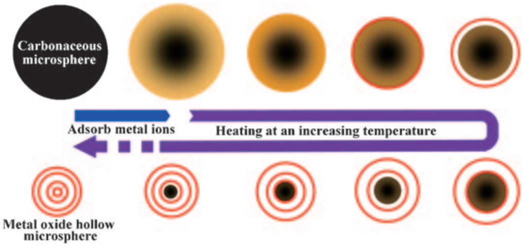

A sphere of many coats: A facile sequential templating process for the general preparation of metal oxide hollow microspheres with multiple shells (red), such as α-Fe_2O_3, Co_3O_4, NiO, CuO, ZnO, and $ZnFe_2O_4$, may open up new opportunities for preparing advanced materials based on complex hollow structures with multipurpose applications.

Thin Films

S. Cho, G. Han, K. Kim, M. M. Sung* ____ **2742 – 2746**

High-Performance Two-Dimensional Polydiacetylene with a Hybrid Inorganic–Organic Structure

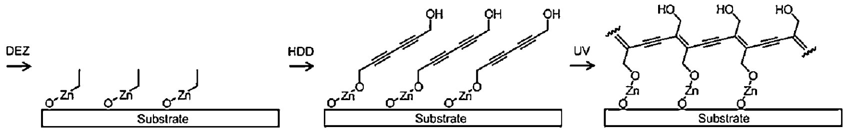

Thin films not thin on the ground: The title films were grown by molecular layer deposition involving repeated sequential adsorption of diethylzinc (DEZ) and hexadiyne diol (HDD) with UV polymerization. The prepared zinc oxide cross-linked polydiacetylene films exhibited good thermal and mechanical stabilities, enhanced carrier mobility ($>1.3\ cm^2V^{-1}s$), and other favorable properties owing to their 2D structures.

Olefin Hydro-metathesis

V. Polshettiwar,* J. Thivolle-Cazat,* M. Taoufik,* F. Stoffelbach, S. Norsic, J.-M. Basset* ____ **2747 – 2751**

"Hydro-metathesis" of Olefins: A Catalytic Reaction Using a Bifunctional Single-Site Tantalum Hydride Catalyst Supported on Fibrous Silica (KCC-1) Nanospheres

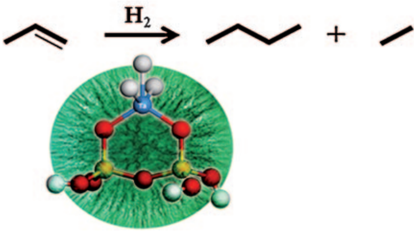

Tantalizing hydrocarbons: Tantalum hydride supported on fibrous silica nanospheres (KCC-1) catalyzes, in the presence of hydrogen, the direct conversion of olefins into alkanes that have higher and lower numbers of carbon atoms (see scheme). This catalyst shows remarkable catalytic activity and stability, with excellent potential of regeneration.

Metallocenes

M. Toganoh, A. Sato, H. Furuta* ____ **2752 – 2755**

Double-Decker Ferrocene-Type Complex of N-Fused Porphyrin: A Model of π-Extended Ferrocene?

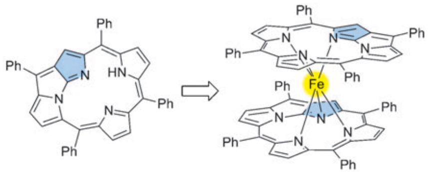

Whopper sandwich: A double-decker ferrocene-type complex with N-fused porphyrinato ligands (see picture) was synthesized from N-fused porphyrin, and its structure and properties were characterized with X-ray crystallographic analysis, variable-temperature ^{1}H NMR spectra, and electrochemical measurements. The unique three-dimensional d–π conjugated system was elucidated with the aid of DFT studies.

Contents

Ring Contraction

A. Y. Hong, M. R. Krout, T. Jensen,
N. B. Bennett, A. M. Harned,
B. M. Stoltz* ______ **2756 – 2760**

Ring-Contraction Strategy for the Practical, Scalable, Catalytic Asymmetric Synthesis of Versatile γ-Quaternary Acylcyclopentenes

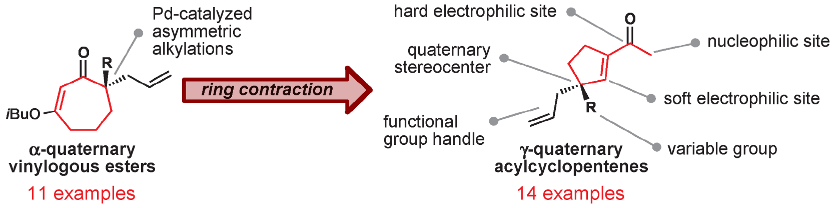

Contraction action! A simple protocol for the catalytic asymmetric synthesis of highly functionalized γ-quaternary acylcyclopentenes (see schematic) in up to 91 % overall yield and 92 % *ee* has been developed. The reaction sequence employs a palladium-catalyzed enantioselective alkylation reaction and exploits the unusual stability of β-hydroxy cycloheptanones to achieve a general and robust method for performing two-carbon ring contractions.

Fluorophore-Binding Proteins

Y. K. Kim, J.-S. Lee, X. Bi, H.-H. Ha,
S. H. Ng, Y.-h. Ahn, J.-J. Lee, B. K. Wagner,
P. A. Clemons, Y.-T. Chang* **2761 – 2763**

The Binding of Fluorophores to Proteins Depends on the Cellular Environment

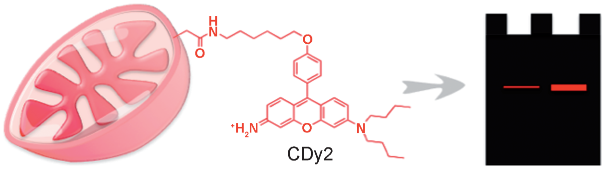

Lighten up! To investigate intracellular binders of myotube-specific probes, a thiol-reactive derivative, CDy2, was prepared. In live cells, the derivative selectively localizes in mitochondria and covalently labels its binding partners.

Carbon Nanotubes

S. Cambré, W. Wenseleers* **2764 – 2768**

Separation and Diameter-Sorting of Empty (End-Capped) and Water-Filled (Open) Carbon Nanotubes by Density Gradient Ultracentrifugation

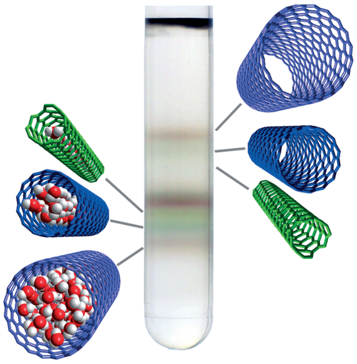

Sorting by spinning: Empty (end-capped) and water-filled (open) carbon nanotubes, which coexist in aqueous solutions, can be separated by density gradient ultracentrifugation (see picture), and the empty tubes allow enhanced diameter sorting. The isolated empty nanotubes possess narrower electronic and vibrational transitions and enhanced quantum efficiences compared to the water-filled nanotubes.

Catalysis

A.-L. Auvinet,
J. P. A. Harrity* ______ **2769 – 2772**

A Nickel-Catalyzed Benzannulation Approach to Aromatic Boronic Esters

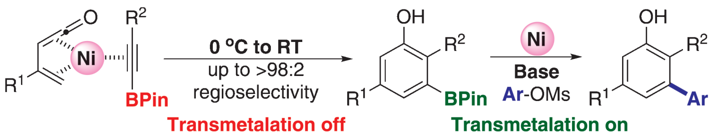

Off and on: A nickel-catalyzed benzannulation of alkynylboronates provides functionalized phenols with high levels of chemo- and regioselectively. While transmetalation of organoboron intermediate to organonickel does not occur during cycloaddition, it is “switched on” by addition of base, thus allowing a one-pot benzannulation and cross-coupling to be realized (see scheme; Pin = pinacolato, Ms = mesyl).

Electrocatalysis

T. Yu, D. Y. Kim, H. Zhang,
Y. Xia* ———— **2773–2777**

Platinum Concave Nanocubes with High-Index Facets and Their Enhanced Activity for Oxygen Reduction Reaction

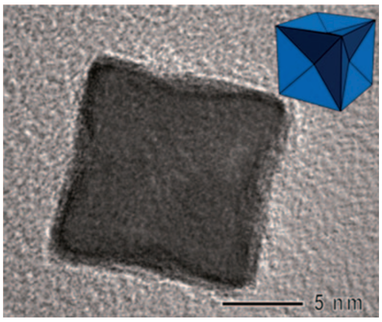

Many facets: A simple synthetic route, which is based on reduction in aqueous solution, results in Pt concave nanocubes (see picture) enclosed by high-index facets such as {510}, {720}, and {830}. The nanocrystals exhibit electrocatalytic activity (per unit surface area) that is 3.5 times higher than the commercial Pt/C catalyst in the oxygen reduction reaction.

Catalytic Hydroboration

Y. Sasaki, Y. Horita, C. Zhong,
M. Sawamura, H. Ito* ———— **2778–2782**

Copper(I)-Catalyzed Regioselective Monoborylation of 1,3-Enynes with an Internal Triple Bond: Selective Synthesis of 1,3-Dienylboronates and 3-Alkynylboronates

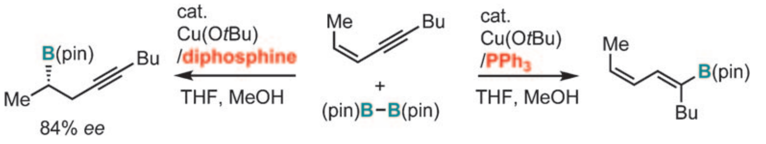

Hooray for hydroboration! The products afforded by the title reaction depend on the substitution pattern on the double bond moiety of 1,3-enyne substrates (see scheme). These types of products, either 1,3-dienylboronates or 3-alkynylboronates, are difficult to obtain by other methods. Interestingly, ligand-controlled borylation was observed with high selectivity in some cases. pin = pinacolato, THF = tetrahydrofuran.

C−F Activation

J. A. Panetier, S. A. Macgregor,*
M. K. Whittlesey* ———— **2783–2786**

Catalytic Hydrodefluorination of Pentafluorobenzene by $[Ru(NHC)(PPh_3)_2(CO)H_2]$: A Nucleophilic Attack by a Metal-Bound Hydride Ligand Explains an Unusual *ortho*-Regioselectivity

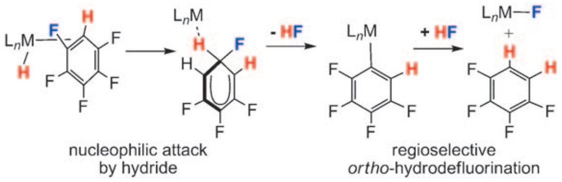

Secret revealed: The mechanism of the catalytic hydrodefluorination of pentafluorobenzene by the N-heterocyclic carbene complex $[Ru(IMes)(PPh_3)_2(CO)H_2]$ has been investigated by DFT calculations. Two sets of novel pathways (concerted and stepwise) have been defined whereby a Ru H ligand can act as a nucleophile at the fluoroarene substrate. The most accessible pathway equates to the formation of 1,2,3,4-$C_6F_4H_2$ and thus accounts for the unusual regioselectivity that is observed experimentally (see scheme).

Bioinspired Synthesis

Y. Wang, L. Zhu, Y. Zhang,
R. Hong* ———— **2787–2790**

Bioinspired and Concise Synthesis of (±)-Stemoamide

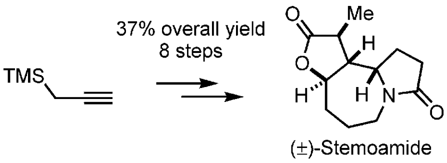

Natural inspiration: A concise total synthesis of (±)-stemoamide was completed in eight steps with a 37% overall yield. A bioinspired N-acyliminium ion cyclization and an unprecedented dynamic ruthenium-catalyzed cyclocarbonylation ensured the high efficiency of the synthesis. A novel silver-mediated cyclization of an allenic alcohol shows potential for the future asymmetric synthesis of the target. TMS = trimethylsilyl.

Nanostructures

D. Wu, R. Liu, W. Pisula, X. Feng,*
K. Müllen* **2791 – 2794**

Two-Dimensional Nanostructures from Positively Charged Polycyclic Aromatic Hydrocarbons

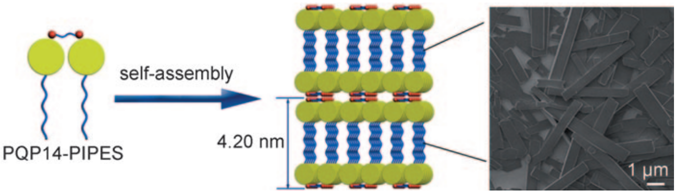

Conducting experiments: Amphiphilic PQP14 complexes self-assemble into two-dimensional (2D) nanostructures in a controlled way by choosing alkyl sulfonates or disulfonates as anions (see picture). The morphologies of these 2D nanostructures significantly affect the ionic conductivity of the mixture of PQP14 complexes and lithium salts, for which the planar aggregates exhibit a conductivity of two orders of magnitude higher than that of the puckered ones.

Biosynthesis Mechanisms

L. Gu, E. B. Eisman, S. Dutta,
T. M. Franzmann, S. Walter,
W. H. Gerwick, G. Skiniotis,
D. H. Sherman* **2795 – 2798**

Tandem Acyl Carrier Proteins in the Curacin Biosynthetic Pathway Promote Consecutive Multienzyme Reactions with a Synergistic Effect

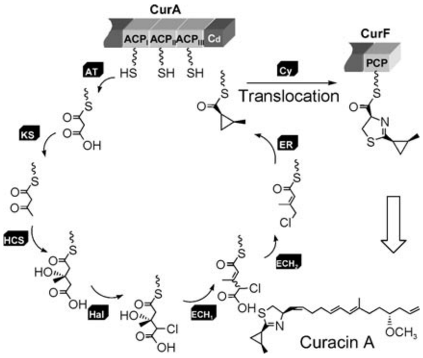

Synergistic gathering: Biochemical studies reveal a highly efficient strategy in biosynthesis to promote consecutive multienzyme reactions. In the curacin A pathway, catalytic efficiency of a multi-step modification process and one-step translocation is significantly enhanced by tandem organization and dimerization of the ACP$_3$ tridomain with an unexpected synergistic effect (see scheme).

Polymer Solar Cells

E. J. Zhou, J. Z. Cong, Q. S. Wei,
K. Tajima,* C. H. Yang,
K. Hashimoto* **2799 – 2803**

All-Polymer Solar Cells from Perylene Diimide Based Copolymers: Material Design and Phase Separation Control

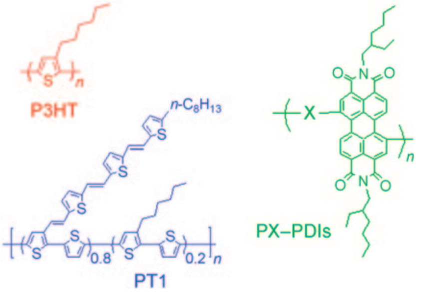

It's all about polymers: All-polymer solar cells (all-PSCs) based on six perylene diimide containing polymers (PX–PDIs) as acceptor materials and two polythiophene derivatives (P3HT and PT1) as donor materials were investigated systematically (see picture). The highest power-conversion efficiency (PCE) of all-PSCs was 2.23 %, one of the highest PCEs of polymer/polymer blend photovoltaic devices reported to date.

Asymmetric Synthesis

Y. Hayashi,* Y. Yasui, T. Kawamura,
M. Kojima, H. Ishikawa **2804 – 2807**

One-Pot Synthesis of Chiral α-Substituted β,γ-Epoxy Aldehyde Derivatives through an Asymmetric Aldol Reaction of Chloroacetaldehyde

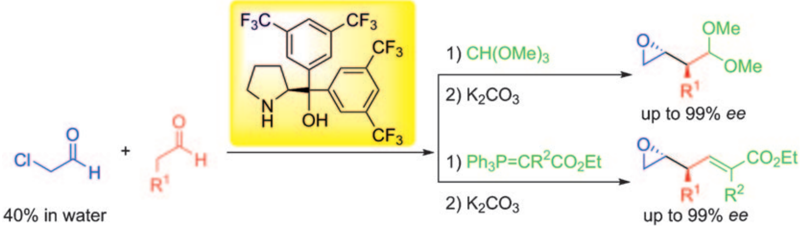

Water is welcome! Chiral α-substituted β,γ-epoxides have been prepared in good yields and with excellent enantioselectivities in a one-pot synthetic procedure. The key reaction of this process, which involves a series of uninterrupted sequential reactions, is an asymmetric aldol reaction of aqueous chloroacetaldehyde mediated by a diarylprolinol derivative (see scheme).

An unprecedented reaction mode of cyanogen bromide has been discovered. Under basic conditions, cyanogen bromide acts as an equivalent of both Br^+ and CN^- to convert enolizable ketones into the corresponding cyanoepoxides in good yields. This unique reaction mode provides new, one-pot access to densely substituted cyanoepoxides from easily available ketones (see scheme).

Cascade Reactions

Z. Li, V. Gevorgyan* ______ 2808 – 2810

Double Duty for Cyanogen Bromide in a Cascade Synthesis of Cyanoepoxides

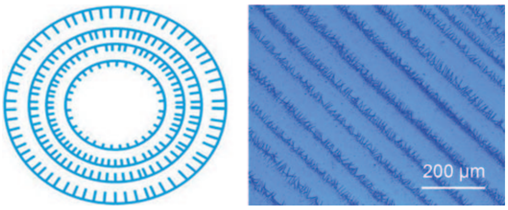

Concentric rings of organic nanowires (see schematic and micrographs) were prepared simply by controlling the evaporation of a droplet of dye solution in a confined space. By adjusting the initial concentration, the density and spacing of the concentric arrays of organic nanowires can be tuned. This facile approach can also be used to produce large-scale organic semiconductor devices with nanowire configuration.

Controlled Evaporation

Z. L. Wang, R. R. Bao, X. J. Zhang,
X. M. Ou, C. S. Lee, J. C. Chang,
X. H. Zhang* ______ 2811 – 2815

One-Step Self-Assembly, Alignment, and Patterning of Organic Semiconductor Nanowires by Controlled Evaporation of Confined Microfluids

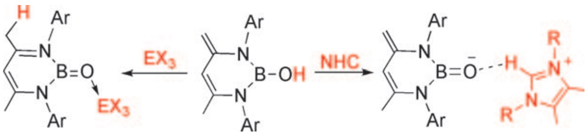

Have it B=Oth ways: Metal-free anionic oxoboranes and Lewis acid stabilized oxoboranes that feature a formal B=O double bond can be conveniently obtained from an N-heterocyclic borinic acid in the presences of N-heterocyclic carbenes (NHCs) and Lewis acids, respectively (see picture).

Oxoboranes

Y. Wang, H.-F. Hu, J.-Y. Zhang,
C.-M. Cui* ______ 2816 – 2819

Comparison of Anionic and Lewis Acid Stabilized N-Heterocyclic Oxoboranes: Their Facile Synthesis from a Borinic Acid

Hunting high and low: A cyanide-bridged rhombic mixed-spin Fe^{II}–Fe^{II} complex that features low-spin (LS) and high-spin (HS) Fe^{II} centers was prepared by self-assembly including the decomposition of SeCN. The structural motif represents a hybrid [2×2]grid/metallocyclic architecture (see picture).

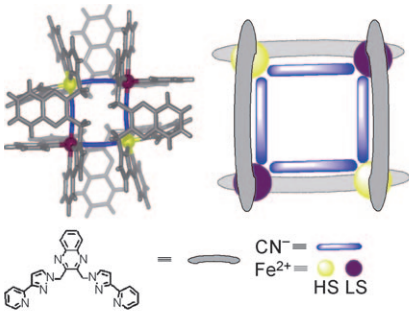

Metallastructures

F. Li, J. K. Clegg, L. Goux-Capes,
G. Chastanet, D. M. D'Alessandro,
J.-F. Létard, C. J. Kepert* ______ 2820 – 2823

A Mixed-Spin Molecular Square with a Hybrid [2×2]Grid/Metallocyclic Architecture

Domino Reactions

H. Ishikawa, M. Honma,
Y. Hayashi* ______ **2824 – 2827**

One-Pot High-Yielding Synthesis of the DPP4-Selective Inhibitor ABT-341 by a Four-Component Coupling Mediated by a Diphenylprolinol Silyl Ether

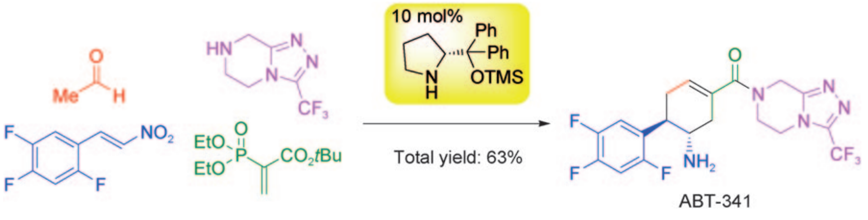

A dream come true: ABT-341 was synthesized in high yield with excellent diastereo- and enantioselectivity in a one-pot process mediated by a diphenylprolinol silyl ether (see scheme; TMS = trimethylsilyl). Thus, an asymmetric Michael reaction, a domino Michael/Horner–Wadsworth–Emmons reaction combined with a retro-aldol reaction, base-catalyzed isomerization, amide-bond formation, and reduction of the nitro group all took place in a single flask.

DNA-Directed Synthesis

A. Erben, T. N. Grossmann,
O. Seitz* ______ **2828 – 2832**

DNA-Triggered Synthesis and Bioactivity of Proapoptotic Peptides

A great leap for an amino acid is enabled by a DNA-triggered reaction which involves the transfer of an aminoacyl group from a donating thioester-linked PNA–peptide hybrid to a peptide–PNA acceptor (see scheme). The formed peptide conjugates acted as antagonists to the X-linked inhibitor of apoptosis protein (XIAP) and allowed reactivation of initiator caspase-9 as well as the executioner caspase-3.

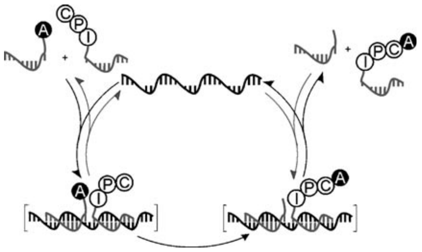

Boron Heterocycles

K. Ansorg, H. Braunschweig,* C.-W. Chiu,
B. Engels,* D. Gamon, M. Hügel,
T. Kupfer, K. Radacki ______ **2833 – 2836**

The Pentaphenylborole–2,6-Lutidine Adduct: A System with Unusual Thermochromic and Photochromic Properties

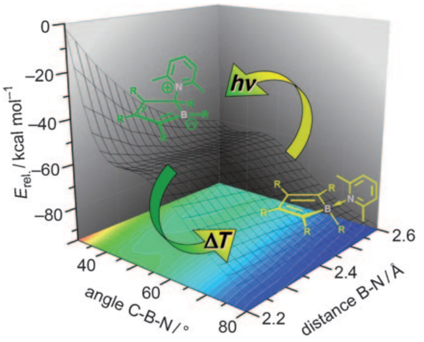

Changing color: The pentaphenylborole–2,6-lutidine adduct **1** has unusual photophysical properties. Cooling a solution of **1** results in the disappearance of the absorption band at 578 nm and a color change from blue to yellow. Irradiation of **1** at low temperatures leads to a migration of lutidine from boron to the adjacent carbon with B=C bond formation and a color change to green.

Amyloid Protofibrils

H. A. Scheidt, I. Morgado, S. Rothemund,
D. Huster,* M. Fändrich* ______ **2837 – 2840**

Solid-State NMR Spectroscopic Investigation of Aβ Protofibrils: Implication of a β-Sheet Remodeling upon Maturation into Terminal Amyloid Fibrils

The secondary structure elements in Aβ protofibrils (see TEM image) were determined at a single residue level by solid-state NMR spectroscopy. The β-sheet elements of the mature fibrils are already preformed in protofibrils, but these regions have to elongate during the conversion into mature fibrils. The data have important implications for understanding the process of fibril formation in general as well as the structural basis of Alzheimer's disease.

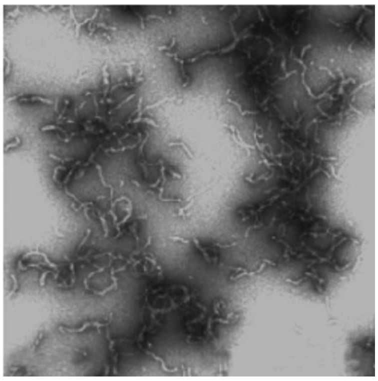

Gas Sensors

M. Hübner, D. Koziej, M. Bauer,
N. Barsan, K. Kvashnina,
M. D. Rossell, U. Weimar,
J.-D. Grunwaldt* ______ **2841 – 2844**

The Structure and Behavior of Platinum in SnO_2-Based Sensors under Working Conditions

Sensor at work: The structure of platinum in a 50 micrometer thin SnO_2 layer is monitored by the combination of a specially designed experimental sensor setup with high-energy-resolution fluorescence-detected X-ray absorption spectroscopy and "range-extended" EXAFS to gain new insights into the local structure of the platinum dopant.

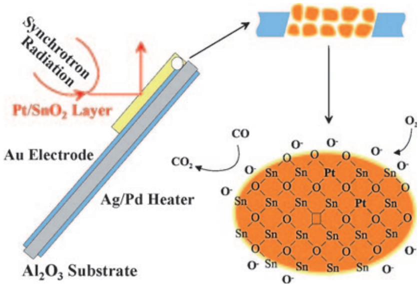

Agostic Alkyl Complexes

W. Scherer,* V. Herz, A. Brück, C. Hauf,
F. Reiner, S. Altmannshofer, D. Leusser,
D. Stalke ______ **2845 – 2849**

The Nature of β-Agostic Bonding in Late-Transition-Metal Alkyl Complexes

Experimental charge density analyses reveal significant differences between the nature of β-agostic bonding in early- and late-transition-metal (M) complexes. For d^n-configurated M alkyl compounds, the β-agostic interaction can be described by a modified Dewar–Chatt–Duncanson model with three σ/π bonding components, whereas one delocalized orbital is sufficient to account for the hyperconjugative stabilization in agostic d^0 systems.

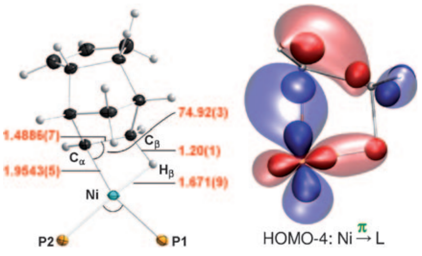

Supramolecular Metal Complexes

M. Albrecht,* E. Isaak, M. Baumert,
V. Gossen, G. Raabe,
R. Fröhlich ______ **2850 – 2853**

"Induced Fit" in Chiral Recognition: Epimerization upon Dimerization in the Hierarchical Self-Assembly of Helicate-type Titanium(IV) Complexes

Undecided! A titanium(IV) triscatecholate bearing chiral ester groups shows different CD spectra in methanol and DMSO. The observation of different stereoisomers lies in the preferred conformation of the side groups in the monomer and dimer, which leads to different chiral induction in the different species.

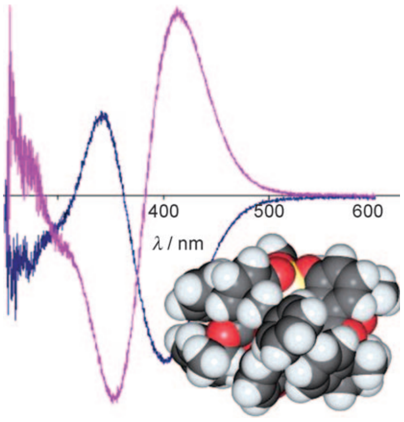

Supporting information is available on www.angewandte.org (see article for access details).

A video clip is available as Supporting Information on www.angewandte.org (see article for access details).

This article is available online free of charge (Open Access).

Service

Spotlight on Angewandte's Sister Journals ______ *2666–2668*

Preview ______ *2855*

Corrigendum

Asymmetric Mannich Reaction of Fluorinated Ketoesters with a Tryptophan-Derived Bifunctional Thiourea Catalyst

X. Han, J. Kwiatkowski, F. Xue,
K.-W. Huang,* Y. Lu* ______ **7604–7607**

Angew. Chem. Int. Ed. **2009**, *48*

DOI 10.1002/anie.200903635

The authors of this Communication (10.1002/anie.200903635) have recognized an error in Figure 1, which was inadvertently replaced by a model structure. The correct Figure 1 is shown below.

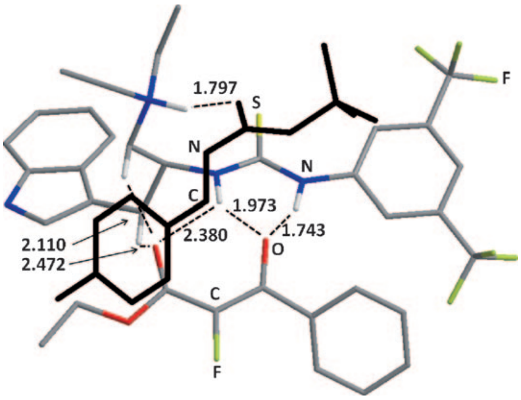

Figure 1. Intermediate **IMa** formed from **1a**, **2a**, and **Trp-1**. Hydrogen-bond distances are given in Å (non-hydrogen-bonded hydrogen atoms were omitted for clarity).

The text which refers to Figure 1 (page 7605, right column) is also incorrect. It should read: “We carried out density functional theory calculations to elucidate the stereochemical outcome of this novel Mannich reaction.[12] Our preliminary efforts were focused on the identification of the structure of the pre-transition-state complex. Complex **IMa** (for the formation of **3a**) was located as the most plausible intermediate. With a C–C bond distance of 3.637 Å, it is ready to undergo the bond-forming step (Figure 1). The diethylamino group of **Trp-1** could first deprotonate **1a** to yield an ammonium group. Nonclassical C–H···O interactions were observed, which might presumably assist the thiourea moiety in binding the resulting ketoenolate. The ammonium group could later direct and bind the incoming imine to bring it into proximity with the ketoenolate in a locked conformation.”
The authors would like to point out that this error does not affect the interpretation of results in the Communication.